Unified description of linear screening in dense plasmas

L. G. Stanton[1,*] and M. S. Murillo[2,†]

[1]*Center for Applied Scientific Computing, Lawrence Livermore National Laboratory, Livermore, California 94550, USA*

[2]*Computational Physics and Methods Group, Los Alamos National Laboratory, Los Alamos, New Mexico 87545, USA*

(Received 10 July 2014; published 6 March 2015; corrected 30 March 2015)

Electron screening of ions is among the most fundamental properties of plasmas, determining the effective ionic interactions that impact all properties of a plasma. With the development of new experimental facilities that probe high-energy-density physics regimes ranging from warm dense matter to hot dense matter, a unified framework for describing dense plasma screening has become essential. Such a unified framework is presented here based on finite-temperature orbital-free density functional theory, including gradient corrections and exchange-correlation effects. We find a new analytic pair potential for the ion-ion interaction that incorporates moderate electronic coupling, quantum degeneracy, gradient corrections to the free energy, and finite temperatures. This potential can be used in large-scale "classical" molecular dynamics simulations, as well as in simpler theoretical models (e.g., integral equations and Monte Carlo), with no additional computational complexity. The new potential theoretically connects limits of Debye-Hückel–Yukawa, Lindhard, Thomas-Fermi, and Bohmian quantum hydrodynamics descriptions. Based on this new potential, we predict ionic static structure factors that can be validated using x-ray Thomson scattering data.

DOI: 10.1103/PhysRevE.91.033104 PACS number(s): 52.27.Gr, 34.20.Cf, 52.25.Kn, 71.10.Ca

I. INTRODUCTION

Accurate modeling of dense plasmas often requires very-large-scale molecular dynamics (MD) simulations. Reaching the mesoscopic scales of nonequilibrium transport can necessitate millions to billions of particles [1]. To achieve these scales while still maintaining a predictive capability, pair potentials that are simple in form (preferably *analytic*), *rigorously derived*, and *wide-ranging* are of immense utility; they are also of use in integral equations, such as the hypernetted chain equations, and in Monte Carlo simulations. Moreover, as MD simulations have as their primary input a potential (or force), it is essential that a deeper understanding is formulated of the physical underpinnings of the plethora of available potentials, which can be derived from Debye-Hückel–Yukawa, Lindhard, Thomas-Fermi, Bohmian hydrodynamic theories, *etc.* [2–4]. This is of particular interest today as new high-energy-density facilities, such as the National Ignition Facility (NIF) and the Linac Coherent Light Source (LCLS), begin generating high-quality data across large regions of parameter space [5,6]. In particular, while plasma screening is well understood at very high temperatures, we desire a description that spans into the warm dense matter (WDM) regime where condensed matter behavior appears; WDM occurs in giant planets, fast ignition experiments, and other laboratory experiments [7]. Insights into plasma screening across orders of magnitude in temperature and density also reconcile issues arising in quantum hydrodynamics (QHD) [8], including recent controversies regarding novel quantum potentials obtained from the Bohmian formulation [9–14].

In this paper, we focus primarily on linear screening. When the screening is describable in terms of a dielectric response of the form $\epsilon(k) = 1 + (\lambda_s k)^{-2}$, one obtains the celebrated Yukawa potential (also known as the Debye-Hückel or screened Coulomb potential):

$$\phi(r) = \frac{Ze}{r} e^{-r/\lambda_s}, \tag{1}$$

where Ze is the impurity charge and λ_s is the screening length. Since the pioneering work of Debye and Hückel [15], the Yukawa form has been applied widely to electrolytes, colloids, and dilute plasmas [3,4]. In a hot, dilute system, the screening length associated with the electrons is given by $\lambda_{\rm D} = \sqrt{k_B T_e/(4\pi e^2 n)}$ [Debye-Hückel (DH) screening], whereas in a dense plasma, it is given more generally by $\lambda_{\rm TF}^{-2} = 4\pi e^2(\partial n/\partial\mu)$ [Thomas-Fermi (TF) screening] to account for degeneracy effects. Here n is the mean electron density, e is the elementary charge, k_B is the Boltzmann constant, T_e is the electron temperature, and μ is the chemical potential. We generalize the Debye-Hückel–Yukawa model to incorporate gradient corrections and quantum exchange-correlation effects in the free energy that extend the Yukawa form toward moderate electron coupling.

The paper is organized as follows. In Sec. II, we derive an analytic generalization of the Yukawa potential to include finite-temperature gradient corrections in the free energy and exchange-correlation effects. An analysis of the potential and numerical results are then presented in Sec. III. In Sec. IV, we compare our model to similar potentials used in the field within the framework of quantum hydrodynamics. Finally, conclusions are presented in Sec. V.

II. MODEL FORMULATION

In this section, we proceed in small steps to illustrate the relative contributions to the overall screening theory. We begin by reviewing the basic TF screening model and its formulation as an orbital-free density functional theory (OF-DFT) to yield a screened potential valid over the entire temperature range. In Sec. II A, we then add a finite-temperature gradient correction to the kinetic energy and find that a qualitatively new functional form emerges

*liam@llnl.gov

†murillo@lanl.gov

 ©2015 American Physical Society

under certain conditions. Finally, in Sec. II B, we include the exchange-correlation (XC) contribution at long wavelengths and obtain XC corrections while retaining an analytic form useful across wide ranges of coupling and degeneracy.

To allow us to focus on linear screening properties, we incorporate the strongly interacting localized states into an effective nuclear charge Z^*e and examine the properties of the weakly interacting "free" states [7]. We use atomic units (i.e., $e = m_e = \hbar = 4\pi\epsilon_0 = 1$) for the remainder of this work. Consider the grand potential [16] for the *free* electrons $n(\mathbf{r})$ in the presence of an external potential produced by the ionic cores, which we write as

$$\Omega = \mathcal{T}[n] + \frac{1}{2}\iint d\mathbf{r}' d\mathbf{r}\, \frac{n(\mathbf{r})n(\mathbf{r}')}{|\mathbf{r}-\mathbf{r}'|} + \int d\mathbf{r}\ [v_{\rm ext}(\mathbf{r}) - \mu]\, n(\mathbf{r}) + \mathcal{F}_{\rm xc}[n], \tag{2}$$

where $\mathcal{T}[n]$ is the kinetic energy functional, the second term is the Hartree (classical) electron-electron interaction, $v_{\rm ext}(\mathbf{r})$ is an external potential arising from the ionic cores, μ is the chemical potential, which ensures charge neutrality, and $\mathcal{F}_{\rm xc}[n]$ is the XC contribution. To obtain an analytic result, we employ an "orbital-free" approach in which several approximations are made for the kinetic energy term; we return to the issue of the XC contribution in Sec. II B. In the long-wavelength limit, the kinetic energy contribution takes the local-density (or TF) form [16] of

$$\mathcal{T} \approx \mathcal{T}_{\rm TF}[n] = \frac{\sqrt{2}}{\pi^2\beta^{5/2}} \int d\mathbf{r} \left[\eta\mathcal{I}_{1/2}(\eta) - \frac{2}{3}\mathcal{I}_{3/2}(\eta)\right], \tag{3}$$

with

$$n(\mathbf{r}) = \frac{\sqrt{2}}{\pi^2\beta^{3/2}}\mathcal{I}_{1/2}[\eta(\mathbf{r})], \tag{4}$$

where the Fermi-Dirac integral of order p is defined as $\mathcal{I}_p(\eta) \equiv \int_0^\infty dx\, x^p/(1+e^{x-\eta})$, and $\beta = 1/T_e$ is the inverse thermal energy of the free electrons (here k_B has been absorbed into the temperature, so that it is expressed in energy units). Upon minimizing the functional (2) with respect to n, by setting $\delta\Omega/\delta n = 0$, we obtain the Euler-Lagrange equation

$$v_{\rm ext}(\mathbf{r}) = \mu - \frac{1}{\beta}\eta(\mathbf{r}) - \int d\mathbf{r}'\, \frac{n(\mathbf{r}')}{|\mathbf{r}-\mathbf{r}'|}. \tag{5}$$

If we next introduce the perturbations $v_{\rm ext} \sim \delta v_{\rm ext}$ and $n \sim n_0 + \delta n$, where n_0 is the mean free electron density, we obtain the susceptibility (in Fourier space)

$$\chi(\mathbf{k}) = \frac{\delta n(\mathbf{k})}{\delta v_{\rm ext}(\mathbf{k})} = \frac{-1}{c_0 + v_{ee}(k)}, \tag{6}$$

with

$$c_0 = (\pi^2\sqrt{2\beta})/\mathcal{I}_{-1/2}(\eta_0), \tag{7}$$

where $v_{ee}(k) = 4\pi/k^2$, $k = |\mathbf{k}|$, and $\eta_0 = \eta(n_0)$ from relation (4). Taking the external potential to be from a collection of point ions yields the relation

$$\delta n(\mathbf{k}) = -v_{ee}(k)\chi(k)\sum_n Z^* e^{i\mathbf{k}\cdot\mathbf{R}_n}, \tag{8}$$

where the ions are located at positions $\mathbf{R}_n$. Using the approximation $n \approx n_0 + \delta n$ and the Poisson equation $\nabla^2\Phi = -4\pi\rho$, we can solve for the total electric potential as

$$\Phi(\mathbf{r}) = \sum_n \phi_n(\mathbf{r} - \mathbf{R}_n), \quad \phi_n(\mathbf{r}) = \frac{Z^*}{r}e^{-r/\lambda_{\rm TF}}, \tag{9}$$

where $r = |\mathbf{r}|$, and the TF screening length can be expressed explicitly as

$$\lambda_{\rm TF}^2 = \frac{c_0}{4\pi} = \frac{\pi\sqrt{2\beta}}{4\mathcal{I}_{-1/2}(\eta_0)}. \tag{10}$$

This well-known result is the dense plasma Yukawa screening potential with $\lambda_{\rm TF}(n_0, T_e)$ as the TF screening length (in the high-temperature limit, this naturally reduces to the Debye length).

Up to this point, the effective ion-ion potential (9) incorporates linear, electron screening in the absence of gradient corrections to the free energy or XC effects, where the screening length is obtained from relations (4) and (10). Accurate Padé approximants to the relevant Fermi integrals and their derivatives and inversions can be found in Refs. [17,18]. Note that while the Yukawa potential captures a great deal of the screening physics over the full temperature range with a simple analytic form, it will exhibit several major failures in the predicted electron screening cloud that are associated with TF theory. Of note are the following: (i) the electron density is singular at the ionic core, (ii) the density decays too rapidly far from an ion, and (iii) the density will always decay monotonically (see for example Chap. 6 in Ref. [19]). All three of of these pathologies are addressed in the next section.

A. Gradient-corrected potential

We now improve the TF result through systematic corrections to the grand potential. As the primary weakness of the TF functional is its treatment of a *uniform* electron gas, we include the finite-temperature Kirzhnits gradient correction [20,21] to the kinetic energy, which we write as

$$\mathcal{T} \approx \mathcal{T}_{\rm TF}[n] + \mathcal{T}_{\rm K}[n, \nabla n], \tag{11}$$

$$\mathcal{T}_{\rm K} = \frac{3\sqrt{2}\pi^2}{8}\lambda\beta^{3/2}\int d\mathbf{r}\, \frac{\mathcal{I}'_{-1/2}(\eta)}{\mathcal{I}^2_{-1/2}(\eta)}|\nabla n|^2, \tag{12}$$

where η is calculated from relation (4). Note that, while we are primarily interested in gradient corrections, we also include a factor of λ to allow the model to span both the true gradient-corrected TF limit ($\lambda = 1/9$) and the traditional von Weizsäcker correction at $T_e = 0$ ($\lambda = 1$); however, all calculations presented in this work use the value $\lambda = 1/9$. Now, repeating the above procedure, we obtain the gradient-corrected susceptibility

$$\chi(k) = \frac{-1}{4\pi\lambda_{\rm TF}^2 + \pi\nu\lambda_{\rm TF}^4 k^2 + v_{ee}(k)}, \tag{13}$$

with

$$\nu = \frac{3\sqrt{8\beta}}{\pi}\lambda\mathcal{I}'_{-1/2}(\eta_0), \tag{14}$$

where the prime in Eq. (14) denotes differentiation with respect to η_0.

The parameter ν characterizes the strength of the gradient correction in the free energy and will obviously depend on the mean density and temperature of the free electrons. For $\nu < 1$, which occurs for large densities and/or temperatures, this form readily admits the analytic potential

$$\phi_n(\mathbf{r}) = \frac{Z^*}{2r}[(1+\alpha)e^{-r/\lambda_-} + (1-\alpha)e^{-r/\lambda_+}], \tag{15}$$

where the various coefficients are calculated as

$$\lambda_\pm^2 = \frac{\nu\lambda_{\rm TF}^2}{2 \pm 2\sqrt{1-\nu}}, \quad \alpha = \frac{1}{\sqrt{1-\nu}}. \tag{16}$$

As expected, the TF-Yukawa (TF-Y) result is returned as $\nu \to 0$, which is equivalent to the high-temperature (or density) limit with $\alpha \to 1, \lambda_+ \to 0$, and $\lambda_- \to \lambda_{\rm TF}$. Naturally, the traditional DH limit is included in the high-temperature limit.

For the case $\nu > 1$, we write $\alpha' = 1/\sqrt{\nu - 1}$ (where $\alpha' \in \mathbb{R}$) and obtain the oscillatory potential

$$\phi_n(r) = \frac{Z^*}{r}[\cos(r/\gamma_-) + \alpha' \sin(r/\gamma_-)]e^{-r/\gamma_+}, \tag{17}$$

where the length scales are given by

$$\gamma_\pm^2 = \frac{\nu\lambda_{\rm TF}^2}{\sqrt{\nu} \pm 1}. \tag{18}$$

Equations (15) and (17) give the *exact* gradient-corrected screening (EGS) potential to linear order in the absence of XC effects.

While Eq. (15) is functionally similar to TF-Y, Eq. (17) is *qualitatively* different, a result directly connected with gradient corrections beyond TF. In the cool, dilute regime, the gradient correction predicts that a weak attraction between the ions is possible, a result consistent with the onset of Friedel oscillations [22,23]. The functional forms of Eqs. (15) and (17) will arise within any model that takes next-order gradient corrections into account [24,25], as they merely add higher powers of k^2 to the denominator of Eq. (13), and here we have obtained the specific coefficients in the warm to hot, dense limit.

In Fig. 1, we compare all three length scales: the two new screening lengths, Eqs. (16) and (18), and the classical Debye-Hückel length $\lambda_{\rm D}$. The qualitative changes seen can be understood as lines cutting through the phase diagram in Fig. 3 and crossing the curve $\lambda_+ = \lambda_-$, which will be discussed later.

Using Eq. (8), we can also calculate the electron densities implied by the various pair potentials. For the traditional TF-Y case, the density fluctuation around a given ion is given by

$$\delta n(r) = \frac{Z^*}{4\pi\lambda_{\rm TF}^2 r} e^{-r/\lambda_{\rm TF}} \tag{19}$$

and has the well-known singularity at the ionic core. Using the EGS potential for both monotonic and oscillatory cases, respectively, the electronic density fluctuation around an ion is

$$\delta n_{\rm mon}(r) = \frac{Z^*\alpha}{4\pi\lambda_{\rm TF}^2 r}[e^{-r/\lambda_-} - e^{-r/\lambda_+}], \tag{20}$$

$$\delta n_{\rm osc}(r) = \frac{Z^*\alpha'}{2\pi\lambda_{\rm TF}^2 r} e^{-r/\gamma_+} \sin(r/\gamma_-). \tag{21}$$

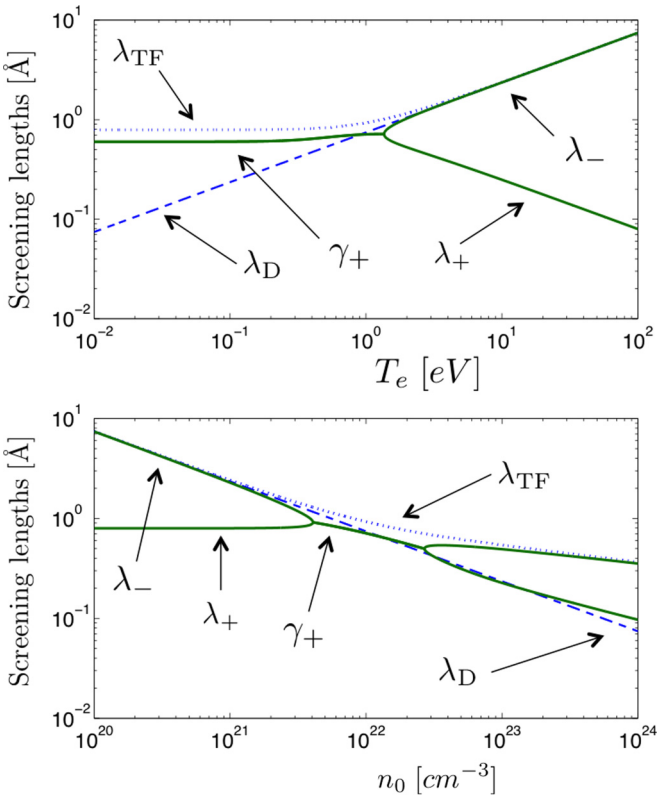

FIG. 1. (Color online) Screening lengths $\lambda_\pm$ and γ_+ for EGS (green, solid line) compared to $\lambda_{\rm TF}$ for TF-Y (blue, dotted line) and $\lambda_{\rm D}$ for DH (blue, dashed line). The top panel shows the lengths as a function of T_e with the fixed mean electron density being $n_0 = 10^{22}\,{\rm cm}^{-3}$, while the bottom panel shows the lengths as a function of n_0 with the fixed temperature $T_e = 1$ eV. The bifurcation points on each EGS curve correspond to the monotonic-oscillatory transition.

From these relations, we can immediately see that the EGS potential correctly predicts a finite cusp at an ionic center for either case, where the monotonic case is shown in Fig. 2. At large distances from the center, it can also be shown that the electron density predicted by the EGS potential will always decay faster than a density resulting from the linearized TF theory. Finally, we observe that the oscillatory potential ($\nu > 1$) yields Friedel-like oscillations in the corresponding density fluctuation. Hence, the inclusion of the gradient correction (12) to obtain Eqs. (15) and (17) is not only a quantitative improvement over the full range of temperatures but also improves three qualitative features lacking in a TF-based model: (i) a finite cusp in the electron screening cloud at an ionic core, (ii) a more rapid decay in the density far from an ion, and (iii) the possibility of Friedel oscillations. Note that while the *correct* cusp condition is not satisfied for either $\lambda = 1$ or $\lambda = 1/9$, λ could be varied to an intermediate value to recover this property.

B. Exchange-correlation effects

The new analytic interionic potentials of Eqs. (15) and (17) were obtained so far in the absence of an XC functional. To address this issue, we must examine how the presence of XC effects alter the coefficients of Eq. (13) and therefore require

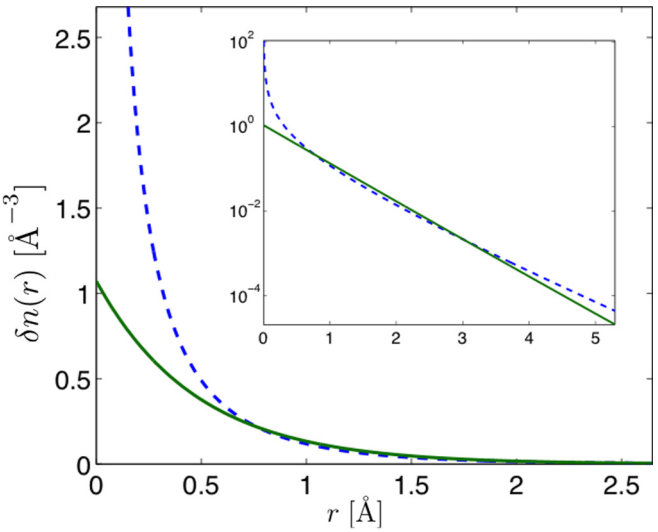

FIG. 2. (Color online) Comparison of free electron density deviations from the mean, n_0, about a point impurity at the origin for TF-Y (blue, dashed) and EGS (green, solid), where $n_0 = 10^{22}\,\mathrm{cm}^{-3}$ and $T_e = 5$ eV. The inset is the same plot on a semilog scale. Note that EGS correctly predicts $\delta n(0)$ to be a finite cusp, and as $r \to \infty$, it predicts a lower electron density. These effects arise due to the fact that the Kirzhnits correction (12) penalizes not only gradients but also low densities.

the long-wavelength expansion of the full response function. We can establish the exact connection between the susceptibility and the local field correction (LFC) $G(k)$ given by

$$\chi(k) = \frac{\chi_0(k)}{1 - v_{ee}(k)\chi_0(k)\,[1 - G(k)]}, \tag{22}$$

where $\chi_0(k)$ is the usual static Lindhard response function

$$\chi_0(k) = -4\int \frac{d\mathbf{p}}{(2\pi)^3}\left[\frac{f_0(\mathbf{p}+\mathbf{k}) - f_0(\mathbf{p})}{|\mathbf{p}+\mathbf{k}|^2 - |\mathbf{p}|^2}\right], \tag{23}$$

with

$$f_0(\mathbf{p}) \equiv [1 + e^{\beta(|\mathbf{p}|^2/2-\mu)}]^{-1}, \tag{24}$$

and the LFC can be written in terms of the XC function through the relation

$$G(k) = -\frac{1}{v_{ee}(k)}\frac{\delta^2 \mathcal{F}_{\mathrm{xc}}[n]}{\delta n(\mathbf{k}')\delta n(\mathbf{k}'')}, \quad k = |\mathbf{k}' - \mathbf{k}''|. \tag{25}$$

The expansion of the inverse Lindhard function can readily be shown to be

$$\chi_0^{-1}(k) \approx -4\pi\lambda_{\mathrm{TF}}^2 - \pi\nu\lambda_{\mathrm{TF}}^4 k^2, \tag{26}$$

and hence the EGS potential can also be viewed as the long-wavelength limit of the Lindhard response theory. Similarly, in this limit, the LFC is formally known to be

$$G(k) \approx \gamma_0 k^2 = \left(1 - \frac{\kappa_0}{\kappa}\right)\frac{\pi k^2}{4k_F}, \tag{27}$$

where the Fermi wave number is $k_F = (3\pi^2 n_e)^{1/3}$, and κ and κ_0 are the isothermal compressibilities for interacting and noninteracting electron gases, respectively [26]. Together, these results yield an exact, long-wavelength susceptibility of the form

$$\chi_{\mathrm{LFC}}(k) = \frac{-1}{4\pi\left(\lambda_{\mathrm{TF}}^2 - \gamma_0\right) + \pi\nu\lambda_{\mathrm{TF}}^4 k^2 + v_{ee}(k)}. \tag{28}$$

Note that this has the *same* functional form as Eq. (13) but with a correction due to the compressibility relation arising from the LFC. The compressibility corrections yield a more accurate potential (up to moderate coupling) but do not change the form. As we can see, the leading-order term (27) enters only into the TF component of the expansion; however, higher-order corrections to $G(k)$ can themselves induce oscillations even in the absence of quantum gradient corrections [27,28]. The coefficients of the EGS potential are hence modified to incorporate this moderate coupling effect as

$$\lambda_\pm^2 \to \frac{\nu\lambda_{\mathrm{TF}}^2}{2b \pm 2\sqrt{b^2 - \nu}}, \quad \alpha \to \frac{b}{\sqrt{b - \nu}}, \tag{29}$$

for the monotonic case, and

$$\gamma_\pm^2 \to \frac{\nu\lambda_{\mathrm{TF}}^2}{\sqrt{\nu} \pm b}, \quad \alpha' \to \frac{b}{\sqrt{\nu - b}}, \tag{30}$$

for the oscillatory case, where $b = 1 - \gamma_0\lambda_{\mathrm{TF}}^{-2}$.

While the compressibility is not known exactly, very accurate predictions have been calculated. For example, the parameter γ_0 can be approximated by neglecting the correlation contributions and using the fit from Refs. [7,29] given by

$$\gamma_0 \approx \tfrac{1}{8}\beta\Theta[h(\Theta) - 2\Theta h'(\Theta)], \tag{31}$$

where the degeneracy parameter is defined as $\Theta \equiv T_e/E_F$, with $E_F = k_F^2/2$, and $h(\Theta)$ is given by

$$h(\Theta) = \frac{N(\Theta)}{D(\Theta)}\tanh(\Theta^{-1}), \tag{32}$$

$$N(\Theta) = 1 + 2.8343\Theta^2 - 0.2151\Theta^3 + 5.2759\Theta^4, \tag{33}$$

$$D(\Theta) = 1 + 3.9431\Theta^2 + 7.9138\Theta^4. \tag{34}$$

III. RESULTS

A. Regimes of validity

The TF-Y model can be viewed as the first-order correction to a purely Coulombic system. As T_e is lowered from infinity, the length scale λ_{TF} becomes finite and eventually comparable to the characteristic length scale of the system [the ion sphere radius, $a_i = (4\pi n_i/3)^{-1/3}$]. When $a_i \sim \lambda_{\mathrm{TF}}$, the approximation of bare Coulomb interactions is no longer valid. This crossover is equivalent to the point at which the number of particles within a Debye sphere has reached unity.

Now that we have the gradient-corrected potential, we can apply the same reasoning to establish a regime of validity for a TF-Y system. Within the framework of the EGS model, λ_- acts as the modified Debye-like screening length, and the next-order length-scale to arise from the gradient correction is λ_+. The TF-Y model should then lose its validity when $\lambda_+ \sim \lambda_-$. In Fig. 3, we have shown both $a_i = \lambda_{\mathrm{TF}}$ and $\lambda_+ = \lambda_-$ in the (n_i, T_e) parameter space; the latter curve being equivalent to $\mathcal{I}'_{-1/2}(\eta_0) = 3\pi\sqrt{T_e/8}$ when $G(k) = 0$. We have chosen to show this with Be and have used a TF fit to approximate Z^* (see Table IV of Ref. [30]). As the white line shows, Coulombic

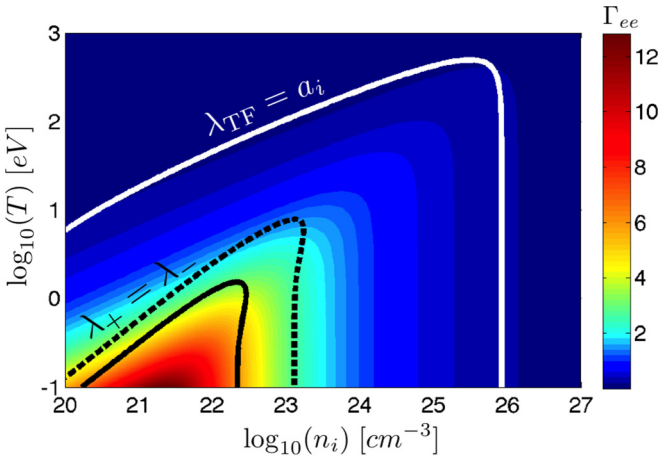

FIG. 3. (Color online) Phase space regions of screening model validity for Be. Unscreened Coulombic interactions lose validity for temperatures and densities below $\lambda_{TF} = a_i$ (white line), and similarly, the Yukawa interaction loses validity below $\lambda_+ = \lambda_-$ (black lines). For the latter condition, we have shown the cases with (dashed, black line) and without (solid, black line) local field corrections. Behind these curves, a color plot of Γ_{ee} is shown to demonstrate regions of strong *e*-*e* coupling.

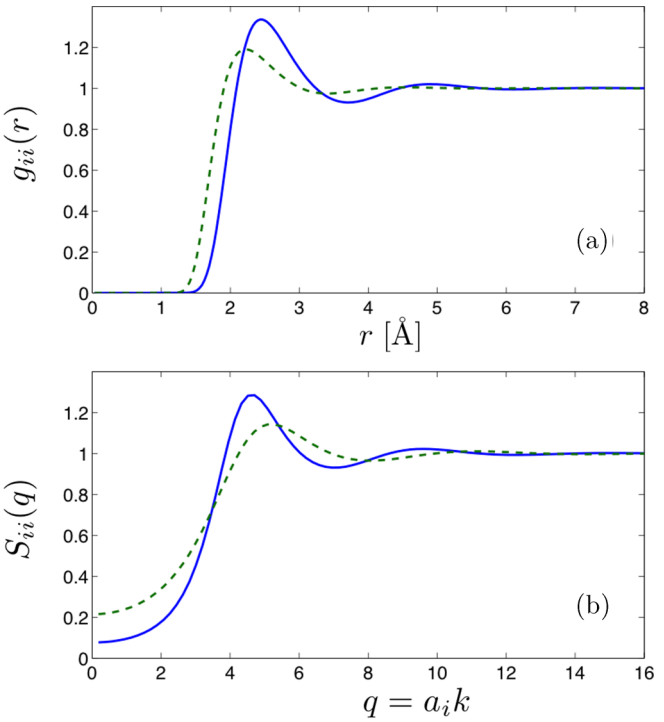

FIG. 4. (Color online) Radial distribution function (a) and static structure factor (b) comparisons between TF-Y (blue, dashed line) and EGS (green, solid line) models for Al. In each case, we have set $Z^* = 3$, $n_i = 6 \times 10^{22}$ cm^{-3}, and $T_e = 0.5$ eV. The EGS potential predicts a lower repulsion between ions than the TF-Y model due to the reduced electron densities near the ionic centers; however, the overall screening effects are enhanced from the diminished densities in the far field.

interactions lose validity to Yukawa interactions which in turn lose validity to the EGS interaction as T_e and n_i decrease (solid black line). We have also included the curve $\lambda_+ = \lambda_-$ with LFCs (dashed black line), which appears to enhance the importance of the gradient corrections. Behind each of these curves, we have additionally plotted a colormap of the electron-electron (*e*-*e*) coupling strength, which is taken as

$$\Gamma_{ee} = \frac{e^2}{a_e \mathcal{T}_e}, \quad a_e = \left(\frac{3}{4\pi n_0}\right)^{1/3}. \tag{35}$$

Here, the electron kinetic energy is approximated using

$$\mathcal{T}_e \approx 2 \int \frac{d\mathbf{p}}{(2\pi)^3} \left(\frac{p^2}{2}\right) f_0(\mathbf{p}), \tag{36}$$

where $f_0(\mathbf{p})$ is the Fermi-Dirac distribution defined in Eq. (24). From the figure, it is clear that the gradient corrections are larger in regions with stronger *e*-*e* coupling.

B. Correlation functions

Finally, we present ion-ion radial distribution functions, $g_{ii}(r)$, and the corresponding static structure factors calculated from the relation

$$S_{ii}(k) = 1 + n h_{ii}(k). \tag{37}$$

Here, $h_{ii}(k)$ is the Fourier transform of the total correlation function defined by $h_{ii}(r) \equiv g_{ii}(r) - 1$. We compute these correlation functions using the Ornstein-Zernike equation

$$h_{ii}(r) = c_{ii}(r) + n \int d\mathbf{r}' h_{ii}(|\mathbf{r} - \mathbf{r}'|) c_{ii}(r') \tag{38}$$

and the hypernetted-chain closure relation

$$g_{ii}(r) = \exp\{h_{ii}(r) - c_{ii}(r) - \beta Z_i \phi_i(r)\}, \tag{39}$$

where $c_{ii}(r)$ is the direct correlation function (see for example Chap. 10.3 in Ref. [31]). The calculations were performed for Al with the ionization taken as the valence $Z^* = 3$ at solid density and $T_e = 0.5$ eV as shown in Fig. 4. As expected, the EGS potential predicts a lower repulsion between ions than the TF-Y model due to the reduced electron densities near the ionic centers; however, in this case, the overall screening effects are enhanced from the diminished densities in the far field.

IV. COMPARISON TO QHD MODELS

Recently, a "novel attractive force" between ions based on a QHD formulation has been derived by Shukla and Eliasson (SE) [9–11]. Despite issues associated with linearized formulations [12], which is our interest here, the Bohmian formulation of QHD predicts an ion-ion potential similar to our Eqs. (15) and (17), albeit from a very different starting point. Unfortunately, the Bohmian formulation cannot be rigorously extended to finite-temperature or include additional contributions in a self-consistent way. The underlying reason for this limitation is that Bohmian QHD arises from a property of single-particle dynamics, which yields the so-called quantum force or potential.

We desire a QHD framework that makes a *direct* connection to the free energy functional, so that we can incorporate the results of this paper, when QHD is needed [32]. Following the QHD formulation of Bloch [33], which was generalized

by Ying [34] within the formalism of DFT, the equations of motion for the quantum fluid are written as

$$\frac{\partial n}{\partial t} + \nabla \cdot (n\mathbf{v}) = 0, \tag{40}$$

$$\frac{\partial \mathbf{v}}{\partial t} + (\mathbf{v} \cdot \nabla)\mathbf{v} = -\nabla\left(\frac{\delta \mathcal{F}}{\delta n}\right), \tag{41}$$

where the free energy $\mathcal{F} = \Omega + \mu \int d\mathbf{r}\, n(\mathbf{r})$ with the grand potential Ω defined in Eq. (2). In equilibrium, these equations obviously yield the Euler-Lagrange equation ($\delta\Omega/\delta n = 0$) for the density; thus all quantum force terms arise naturally and self-consistently through the free energy for a finite-temperature many-body system. The equilibrium linear response of Blochian QHD is therefore consistent with our formulation.

We can now examine in detail the SE potential within the context of a free energy. If we neglect the XC contribution and evaluate our expression (13) at zero temperature and for $\lambda = 1$, we do recover the Bohmian QHD prediction, revealing that Bohmian QHD is equivalent to the TF model with the von Weizsäcker correction. This limiting case is consistent with the fact that von Weizsäcker [35] originally derived his functional to describe one-electron systems (or, opposite-spin, two-electron systems), and it is therefore not straightforward to extend to finite-temperature many-body systems. Thus, our potentials (15) and (17), being consistent with a QHD theory of the forms (40) and (41) that includes the free energy, greatly improves upon the SE potential. Perhaps most importantly, it also reveals that the SE potential is not "novel" in the sense that any correctly formulated linear screening potential should have the properties we have discussed, like finite electron densities or the possibility of oscillations, which lead to an attractive potential.

V. CONCLUSION

In summary, we have connected disparate viewpoints of linear screening in dense plasmas, including Debye-Hückel–Yukawa, Lindhard, and Bohmian QHD models. By formulating the screening problem in terms of DFT and response functions, we are able to systematically include corrections that incorporate Coulomb coupling and quantum degeneracy effects. We have shown that coupling corrections can be included directly through the local field correction (or equivalently the XC potential) in the long-wavelength limit without changing the functional form of the Yukawa potential. Furthermore, gradient corrections, which are either quantum or short-wavelength coupling in nature, also yield an analytic, ion-ion potential. This effective potential, which is represented analytically in either Eq. (15) or (17) depending on the size of the parameter ν in Eq. (14), improves the fidelity of the Yukawa model, correctly predicts a finite cusp in the electron density at ionic cores, and allows for the onset of Friedel oscillations without compromising any computational complexity in the model.

By comparing our results in the context of "Blochian" QHD [34] (which naturally incorporates self-consistent many-body physics, including exchange correlation, gradient corrections, and finite temperatures) to those derived from the "Bohmian" QHD (which is derived from a one-particle picture), we find that an ion-ion potential from Blochian QHD (equivalent to EGS) should be favored over SE and any other Bohm-like formulation, and hence EGS supersedes SE. An important next step beyond this work is to numerically validate the predictions with nonlinear screening models and experimental measurements of the structure factor.

ACKNOWLEDGMENTS

This work was performed under the auspices of the US Department of Energy by Lawrence Livermore National Laboratory under Contract No. DE-AC52-07NA27344 and by Los Alamos National Laboratory under Contract No. DE-AC52-06NA25396.

[1] F. R. Graziani, V. S. Batista, L. X. Benedict, J. I. Castor, H. Chen, S. N. Chen, C. A. Fichtl, J. N. Glosli, P. E. Grabowski, A. T. Graf *et al.*, Large-scale molecular dynamics simulations of dense plasmas: The Cimarron project, High Energy Density Phys. **8**, 105 (2012).

[2] C. Niedermeier and K. Schulten, Molecular dynamics simulations in heterogeneous dielectrica and Debye-Hückel media—Application to the protein bovine pancreatic trypsin inhibitor, Mol. Simul. **8**, 361 (1992).

[3] J. Barrat, J. Hansen, and H. Totsuji, Collective modes and single-particle motion in Yukawa fluids near freezing, J. Phys. C **21**, 4511 (1988).

[4] K. Kremer, M. O. Robbins, and G. S. Grest, Phase diagram of Yukawa systems: Model for charge-stabilized colloids, Phys. Rev. Lett. **57**, 2694 (1986).

[5] O. Hurricane, D. Callahan, D. Casey, P. Celliers, C. Cerjan, E. Dewald, T. Dittrich, T. Döppner, D. Hinkel, L. B. Hopkins *et al.*, Fuel gain exceeding unity in an inertially confined fusion implosion, Nature (London) **506**, 343 (2014).

[6] C. Bostedt, J. Bozek, P. Bucksbaum, R. Coffee, J. Hastings, Z. Huang, R. Lee, S. Schorb, J. Corlett, P. Denes *et al.*, Ultra-fast and ultra-intense x-ray sciences: First results from the linac coherent light source free-electron laser, J. Phys. B **46**, 164003 (2013).

[7] M. S. Murillo, J. Weisheit, S. B. Hansen, and M. W. C. Dharma-Wardana, Partial ionization in dense plasmas: Comparisons among average-atom density functional models, Phys. Rev. E **87**, 063113 (2013).

[8] D. K. Ferry and J.-R. Zhou, Form of the quantum potential for use in hydrodynamic equations for semiconductor device modeling, Phys. Rev. B **48**, 7944 (1993).

[9] P. K. Shukla and B. Eliasson, Novel attractive force between ions in quantum plasmas, Phys. Rev. Lett. **108**, 165007 (2012).

[10] P. K. Shukla and B. Eliasson, Erratum: Novel attractive force between ions in quantum plasmas, Phys. Rev. Lett. **108**, 219902(E) (2012).
[11] P. Shukla and B. Eliasson, Erratum: Novel attractive force between ions in quantum plasmas, Phys. Rev. Lett. **109**, 019901(E) (2012).
[12] M. Bonitz, E. Pehlke, and T. Schoof, Attractive forces between ions in quantum plasmas: Failure of linearized quantum hydrodynamics, Phys. Rev. E **87**, 033105 (2013).
[13] P. K. Shukla, B. Eliasson, and M. Akbari-Moghanjoughi, Comment on attractive forces between ions in quantum plasmas: Failure of linearized quantum hydrodynamics, Phys. Rev. E **87**, 037101 (2013).
[14] M. Bonitz, E. Pehlke, and T. Schoof, Reply to comment on attractive forces between ions in quantum plasmas: Failure of linearized quantum hydrodynamics, Phys. Rev. E **87**, 037102 (2013).
[15] P. Debye and E. Hückel, The theory of electrolytes. I. The lowering of the freezing point and related occurrences, Phys. Z. **24**, 185 (1923).
[16] N. D. Mermin, Thermal properties of the inhomogeneous electron gas, Phys. Rev. **137**, A1441 (1965).
[17] R. G. Dandrea, N. W. Ashcroft, and A. E. Carlsson, Electron liquid at any degeneracy, Phys. Rev. B **34**, 2097 (1986).
[18] H. Antia, Rational function approximations for Fermi-Dirac integrals, Astrophys. J. Suppl. Ser. **84**, 101 (1993).
[19] R. G. Parr and R. G. P. W. Yang, *Density-Functional Theory of Atoms and Molecules* (Oxford University Press, London, 1989).
[20] D. Kirzhnits, Quantum corrections to the Thomas-Fermi equation, Soviet Phys. JETP **5**, 64 (1957).
[21] F. Perrot, Gradient correction to the statistical electronic free energy at nonzero temperatures: Application to equation-of-state calculations, Phys. Rev. A **20**, 586 (1979).
[22] J. Friedel, XIV. The distribution of electrons round impurities in monovalent metals, Philos. Mag. **43**, 153 (1952).
[23] J. Friedel, Electronic structure of primary solid solutions in metals, Adv. Phys. **3**, 446 (1954).
[24] I. Nagy, A. Arnau, P. M. Echenique, and K. Ladányi, Stopping power of a finite-temperature electron gas for slow unit charges, Phys. Rev. A **43**, 6038 (1991).
[25] K. Ladányi, I. Nagy, and B. Apagyi, Partially linearized Thomas-Fermi-Weizsäcker theory for screening and stopping of charged particles in jellium, Phys. Rev. A **45**, 2989 (1992).
[26] K. Nagao, S. A. Bonev, and N. W. Ashcroft, Cusp-condition constraints and the thermodynamic properties of dense hot hydrogen, Phys. Rev. B **64**, 224111 (2001).
[27] P. Hopkins, A. J. Archer, and R. Evans, Asymptotic decay of pair correlations in a Yukawa fluid, Phys. Rev. E **71**, 027401 (2005).
[28] P. Hopkins, A. Archer, and R. Evans, Pair-correlation functions and phase separation in a two-component point Yukawa fluid, J. Chem. Phys. **124**, 054503 (2006).
[29] F. Perrot and M. W. C. Dharma-Wardana, Exchange and correlation potentials for electron-ion systems at finite temperatures, Phys. Rev. A **30**, 2619 (1984).
[30] R. More, Pressure ionization, resonances, and the continuity of bound and free states, Adv. At. Mol. Phys. **21**, 305 (1985).
[31] J.-P. Hansen and I. R. McDonald, *Theory of Simple Liquids* (Elsevier, Amsterdam, 1990).
[32] J. Vranjes, B. P. Pandey, and S. Poedts, On quantum plasma: A plea for a common sense, Europhys. Lett. **99**, 25001 (2012).
[33] F. Bloch, Stopping power of atoms with several electrons, Z. Phys. **81**, 363 (1933).
[34] S. Ying, Hydrodynamic response of inhomogeneous metallic systems, Nuovo Cimento B, Series 11 **23**, 270 (1974).
[35] C. V. Weizsäcker, Zur theorie der kernmassen, Z. Phys. A: Hadrons Nucl. **96**, 431 (1935).